Journal of Computational Physics 228 (2009) 7634–7642

Contents lists available at ScienceDirect

Journal of Computational Physics

journal homepage: www.elsevier.com/locate/jcp

Robust HLLC Riemann solver with weighted average flux scheme for strong shock

Sung Don Kim [a], Bok Jik Lee [a], Hyoung Jin Lee [a], In-Seuck Jeung [a,b,*]

[a] School of Mechanical and Aerospace Engineering, Seoul National University, Seoul 151-744, Republic of Korea
[b] Institute of Advanced Aerospace Technology, Seoul National University, Seoul 151-744, Republic of Korea

ARTICLE INFO

Article history:
Received 14 April 2009
Received in revised form 6 July 2009
Accepted 15 July 2009
Available online 23 July 2009

Keywords:
HLLC scheme
HLL scheme
WAF scheme
Shock instability
Switching function
HLLC–HLL

ABSTRACT

Many researchers have reported failures of the approximate Riemann solvers in the presence of strong shock. This is believed to be due to perturbation transfer in the transverse direction of shock waves. We propose a simple and clear method to prevent such problems for the Harten–Lax–van Leer contact (HLLC) scheme. By defining a sensing function in the transverse direction of strong shock, the HLLC flux is switched to the Harten–Lax–van Leer (HLL) flux in that direction locally, and the magnitude of the additional dissipation is automatically determined using the HLL scheme. We combine the HLLC and HLL schemes in a single framework using a switching function. High-order accuracy is achieved using a weighted average flux (WAF) scheme, and a method for v-shear treatment is presented. The modified HLLC scheme is named HLLC–HLL. It is tested against a steady normal shock instability problem and Quirk's test problems, and spurious solutions in the strong shock regions are successfully controlled.

1. Introduction

The approximate Riemann solvers are popular shock capturing methods and are widely used in computational studies for high speed flows. However, many researchers have reported failing cases using these schemes. Quirk reported a number of cases in which the Riemann solvers can give unphysical results in multidimensional flows [1]. He described the limitations of the Riemann solvers with respect to shock-capturing properties, and cataloged their failings including expansion shock, negative internal energy, slowly-moving shock, the carbuncle phenomenon, kinked Mach stem, and odd–even decoupling. So-called shock instability, which is a numerical instability in multidimensional flow and the nonexistence of a solution for strong expansion flow, are major problems in such failings.

Researchers have shown that Riemann solvers, which can resolve the contact and shear waves exactly, have such problems in the vicinity of strong shock waves. Quirk suggested a strategy to use combined fluxes so that a dissipative approach, such as the Harten–Lax–van Leer-Einfeldt (HLLE) scheme, can be used in the shock region [1]. Liou analyzed several Riemann solvers by expressing numerical fluxes in terms of mass flux. He defined the dissipative terms in the mass flux of each scheme, and identified the dissipative terms responsible for shock instability [2]. Liou controlled the magnitude of wave speed $|\lambda_2|$ across the contact discontinuity in the Roe scheme to make the pressure difference term have zero value in the dissipative terms of the mass flux. For a strong expansion condition, Quirk also used the HLLE scheme to eliminate the expansion shock appearance in a supersonic corner flow test problem.

* Corresponding author. Address: School of Mechanical and Aerospace Engineering, Seoul National University, Seoul 151-744, Republic of Korea. Tel.: +82 2 880 7387; fax: +82 2 887 2662.
E-mail address: enjis@snu.ac.kr (I.-S. Jeung).

0021-9991/$ - see front matter © 2009 Elsevier Inc. All rights reserved.
doi:10.1016/j.jcp.2009.07.006

The Godunov method can find a solution to the Riemann problem which may be the exact solution or an approximate solution. In the Euler equations, the solution of the local Riemann problem consists of two nonlinear waves (shock or rarefaction waves) and contact discontinuity. Therefore, there are four separate constant states. Harten, Lax, and van Leer presented a direct approximation of the numerical flux to compute Godunov flux [3]. The resulting Harten–Lax–van Leer (HLL) Riemann solver is very efficient and robust. It has an entropy satisfaction property, resolves isolated shock exactly, and preserves positivity [3–5]. The main drawback of the HLL scheme is that it cannot resolve contact discontinuity exactly. Toro, Spruce, and Speares presented a two-state HLL scheme in which the missing contacts and shear waves are restored [4,6]. The resulting Harten–Lax–van Leer contact (HLLC) scheme preserves the entropy satisfaction property of the HLL scheme [4]. Batten et al. showed that the HLLC scheme is positively conservative [7]. The HLLC scheme is the simplest solver to preserve shock, contact, and shear waves exactly. Since the HLL and HLLC schemes hold the entropy satisfaction property and positivity, we focused our interests on shock instability in the vicinity of strong shocks.

Researchers have shown that shock instability is strongly related to the resolution of contact and shear waves. We have proposed a control method of flux difference across the contact for strong shock and expansion flows [8]. In this paper, we provide a simple and clear way of adding dissipation to the HLLC scheme to remedy the numerical shock instability problem. Defining and using a sensing method for the transverse direction of strong shocks, the HLLC scheme is switched to the HLL scheme and the magnitude of the additional dissipation is automatically determined. Since the HLL scheme can resolve isolated shock exactly, local application of the dissipative HLL scheme has no adverse effect on the overall resolution of flow fields. High-order accuracy is achieved using the weighted average flux (WAF) scheme [4,9–12], and implementation of the proposed method using the WAF scheme is presented.

2. HLL and HLLC Riemann solvers with WAF scheme

2.1. HLL and HLLC schemes

The HLL Riemann solver assumes a single constant state between two nonlinear waves (shock or rarefaction) [3,4]. This assumption averages the spatial variations across the contact discontinuity resulting in a smeared solution of contact and shear waves [4]. The HLLC scheme is a modification of the HLL scheme wherein the missing contacts and shear waves are restored [4,6].

The HLL intercell flux is written as [3,4]

$$\mathbf{F}^{HLL}_{\mathbf{i+1/2}} = \begin{cases} \mathbf{F_L}, & 0 \leqslant S_L \\ \mathbf{F}_{*\mathbf{L}} = \mathbf{F_L} + S_L\left(\mathbf{U}^{HLL} - \mathbf{U_L}\right), & S_L \leqslant 0 \leqslant S_* \\ \mathbf{F}_{*\mathbf{R}} = \mathbf{F_R} - S_R\left(\mathbf{U_R} - \mathbf{U}^{HLL}\right), & S_* \leqslant 0 \leqslant S_R \\ \mathbf{F_R}, & 0 \geqslant S_R \end{cases}, \tag{1}$$

where S_L is the smallest wave speed and S_R is the largest wave speed. The subscripts L and R imply the left and right values at the cell interface, respectively. The subscripts $^*L$ and $^*R$ imply the left and right values at the contact discontinuity between two nonlinear waves, respectively.

The single constant state (star region) vector $\mathbf{U}^{HLL}$ is the average of the exact Riemann problem between the slowest and fastest waves [3,4]:

$$\mathbf{U}^{HLL} = \frac{S_R\mathbf{U_R} - S_L\mathbf{U_L} + \mathbf{F_L} - \mathbf{F_R}}{S_R - S_L}. \tag{2}$$

Because the HLL scheme assumes a two-wave system, $\mathbf{F}_{*\mathbf{L}}$ and $\mathbf{F}_{*\mathbf{R}}$ are same as HLL flux $\mathbf{F}^{HLL}$:

$$\mathbf{F}^{HLL} = \frac{S_R\mathbf{F_L} - S_L\mathbf{F_R} + S_RS_L(\mathbf{U_R} - \mathbf{U_L})}{S_R - S_L}. \tag{3}$$

The HLLC intercell flux is written as [4,6]

$$\mathbf{F}^{HLLC}_{\mathbf{i+1/2}} = \begin{cases} \mathbf{F_L}, & 0 \leqslant S_L \\ \mathbf{F}_{*\mathbf{L}} = \mathbf{F_L} + S_L(\mathbf{U}_{*\mathbf{L}} - \mathbf{U_L}), & S_L \leqslant 0 \leqslant S_* \\ \mathbf{F}_{*\mathbf{R}} = \mathbf{F_R} - S_R(\mathbf{U_R} - \mathbf{U}_{*\mathbf{R}}), & S_* \leqslant 0 \leqslant S_R \\ \mathbf{F_R}, & 0 \geqslant S_R \end{cases} \tag{4}$$

$\mathbf{U}_{*\mathbf{L}}$ and $\mathbf{U}_{*\mathbf{R}}$ are the conserved variable vectors in the star region separated by the contact. $\mathbf{F}_{*\mathbf{L}}$ and $\mathbf{F}_{*\mathbf{R}}$ are obtained by applying Rankine-Hugoniot conditions across each wave [4,6].

In the HLLC scheme, variables of states in the star region are obtained with jump conditions across each wave as described by [4,6]:

$$\mathbf{U}_{*\mathbf{K}} = \rho_K \left(\frac{S_K - u_{nK}}{S_K - S_*} \right) \begin{bmatrix} 1 \\ S_* \\ u_{tK} \\ \frac{E_K}{\rho_K} + (S_* - u_{nK}) \left[S_* + \frac{p_K}{\rho_K (S_K - u_{nK})} \right] \end{bmatrix}, \quad K = L \text{ or } R, \tag{5}$$

where the subscripts n and t represent the normal and tangential velocity components, and S_* is the middle wave speed.

To compute wave speeds S_L, S_R, and S_*, the pressure-velocity based wave estimations presented by Toro [4] are used to estimate the shock and the rarefaction waves accurately. More detailed expressions are presented in [4]. Einfeldt proposed wave speeds motivated by the Roe-averaged values $\tilde{u}_n$ and $\tilde{a}$ [5]. Using the modified wave speeds, the HLL scheme is often called the HLLE scheme [4,5,13].

2.2. Finite volume method for non-Cartesian domain

We use the finite volume approach for solving multidimensional problems. The solution is updated including all the intercell fluxes in a single step. An important property of the Euler equation is the rotational invariance. For the non-Cartesian domain, the original conserved variable vector is rotated to the direction normal to the cell interface. Then we apply the local Riemann problem at the rotated frame. In the rotated frame, the local Riemann problem becomes a one-dimensional system [4]. The resulting numerical flux is rotated back to obtain the required intercall flux at each side. The second-order upwind finite volume scheme is achieved using the WAF approach.

2.3. Weighted average flux (WAF) approach

The WAF scheme is the second-order extension of the Godunov first-order upwind method. WAF is second-order accurate in space and time [4,9–12]. In the WAF scheme, intercell flux is represented by an integral average of the physical flux across the full structure of the solution of a local Riemann problem. Since the states between waves are constant, this integral results in the sum of the fluxes at each constant state with weight [4].

The resulting WAF is [4]

$$\mathbf{F}_{\mathbf{i+1/2}} = \sum_{k=1}^{N+1} \beta_k \mathbf{F}^{(\mathbf{k})}_{\mathbf{i+1/2}}, \quad k = 1, \ldots, 4, \tag{6}$$

where N is the number of waves in the Riemann fan.

Weights β_k are expressed in terms of the wave speed S_k as [4]

$$\begin{aligned} &\beta_k = \tfrac{1}{2}(c_k - c_{k-1}) \\ &c_k = \tfrac{\Delta t S_k}{\Delta x}, \quad c_k = \text{Courant number for wave } k \text{ of speed } S_k. \end{aligned} \tag{7}$$

An alternative form of the flux can be rearranged as [1]

$$\mathbf{F}_{\mathbf{i+1/2}} = \frac{1}{2}(\mathbf{F}_{\mathbf{i}} + \mathbf{F}_{\mathbf{i+1}}) - \frac{1}{2} \sum_{k=1}^{N} c_k \Delta \mathbf{F}^{(\mathbf{k})}_{\mathbf{i+1/2}}. \tag{8}$$

Because the WAF scheme is second-order accurate, spurious oscillations appear in the vicinity of a high gradient. The TVD modification of the WAF flux with limiter function $\phi^{(k)}_{i+1/2}$ is written as [4]

$$\mathbf{F}_{\mathbf{i+1/2}} = \frac{1}{2}(\mathbf{F}_{\mathbf{i}} + \mathbf{F}_{\mathbf{i+1}}) - \frac{1}{2} \sum_{k=1}^{N} sign(c_k) \phi^{(k)}_{i+1/2} \Delta \mathbf{F}^{(\mathbf{k})}_{\mathbf{i+1/2}}, \tag{9}$$

where

$$\phi^{(k)}_{i+1/2} = \phi_{i+1/2}\left(r^{(k)}\right). \tag{10}$$

The flow parameter $r^{(k)}$ is defined by [4]

$$r^{(k)} = \begin{cases} \Delta q^{(k)}_{i-1/2} / \Delta q^{(k)}_{i+1/2}, & c_k > 0 \\ \Delta q^{(k)}_{i+3/2} / \Delta q^{(k)}_{i+1/2}, & c_k < 0. \end{cases} \tag{11}$$

For the flow parameter, ρ is selected for a single quantity q [4]. For the limiter function $\phi^{(k)}_{i+1/2}$, the MINBEE (Minmod) limiter is used [4]. The relation between the WAF limiter function and the conventional limiter $\psi^{(k)}_{i+1/2}$ is expressed as [4]

$$\phi^{(k)}_{i+1/2} = 1 - (1 - |c_k|)\psi^{(k)}_{i+1/2}. \tag{12}$$

2.4. Application of WAF to the HLL and HLLC schemes

The WAF scheme can be applied directly to the HLL and HLLC approximate Riemann solvers. In using the HLL or HLLE scheme, the second wave jumps are neglected; hence, there is no difference across the contact and shear waves.

The numerical flux of the HLLC scheme at the intercell boundary is given as [4]

$$\mathbf{F}_{\mathbf{i+1/2}}^{HLLC,WAF} = \frac{1}{2}(\mathbf{F_L} + \mathbf{F_R}) - \frac{1}{2}\begin{bmatrix} sign(c_1)\phi^{(1)}(\mathbf{F}_{*\mathbf{L}} - \mathbf{F_L}) \\ +sign(c_2)\phi^{(2)}(\mathbf{F}_{*\mathbf{R}} - \mathbf{F}_{*\mathbf{L}}) \\ +sign(c_3)\phi^{(3)}(\mathbf{F_R} - \mathbf{F}_{*\mathbf{R}}) \end{bmatrix}. \tag{13}$$

The HLL and HLLE schemes can be expressed in a similar manner:

$$\mathbf{F}_{\mathbf{i+1/2}}^{HLL/HLLE,WAF} = \frac{1}{2}(\mathbf{F_L} + \mathbf{F_R}) - \frac{1}{2}\begin{bmatrix} sign(c_1)\phi^{(1)}(\mathbf{F}_{*\mathbf{L}} - \mathbf{F_L}) \\ +0 \\ +sign(c_3)\phi^{(3)}(\mathbf{F_R} - \mathbf{F}_{*\mathbf{R}}) \end{bmatrix}. \tag{14}$$

In the HLL and HLLE schemes, $\mathbf{F}_{*\mathbf{L}}$ and $\mathbf{F}_{*\mathbf{R}}$ have the same expressions as those of the HLLC scheme, and data $\mathbf{U}_{*\mathbf{L}}$ and $\mathbf{U}_{*\mathbf{R}}$ have the same values as $\mathbf{U}^{HLL}$.

3. Shock instability and its cure

Quirk concluded that any Godunov scheme built upon a single Riemann solver has shortcomings and sometimes fails [1]. He suggested a combination method with a dissipative scheme. Liou suggested that the cause of such failings can be described as a transverse numerical instability associated with the shock wave, and called it "shock instability" [2].

Liou analyzed the structure of the numerical diffusivity of several numerical flux schemes [2]. He confirmed that the root of the shock instability is the dissipative pressure term $D^{(p)}$ in the mass flux. Liou presented the following lemma: "A scheme having the property $D^{(p)} = 0$ in the mass flux is a shock-stable scheme." By Liou's analysis, the HLLE scheme has the property of $D^{(p)} = 0$. Pandolfi and D'Ambrosio reported that "methods that explicitly deal with the contact surface display a clear evidence of carbuncle phenomenon; if the interaction is very weak, or totally ignored, no carbuncle instability occurs." [14].

To investigate the property of the pressure dissipation term of the HLLC scheme, the numerical mass flux expression is applied to the HLLCE scheme. However, the HLLC scheme does not fit in the general mass flux form of Liou. Hence, mass flux is only used in the continuity equation. Detailed expressions of the mass flux for the HLLC scheme is described in [8] and the resulting dissipation term of the continuity equation is expressed as

$$D_{(continuity)}^{HLLC} = A\rho_L \frac{S_* - u_{nL}}{S_L - S_*} + B\rho_R \frac{S_* - u_{nR}}{S_R - S_*}, \tag{15}$$

where constant A and B are presented in [8]. As shown in Eq. (15), there is no pressure difference term in the whole dissipation term. However, the middle wave speed S_* contains a pressure difference term as follows:

$$\frac{1}{\rho_L(S_L - u_{nL}) - \rho_R(S_R - u_{nR})}\Delta p. \tag{16}$$

The estimated middle wave speed contains non-zero pressure difference term and is used for the conserved variable vectors $\mathbf{U}_{*\mathbf{L}}$ and $\mathbf{U}_{*\mathbf{R}}$ in the star region (see Eq. (5)). Therefore, alternative forms of $\mathbf{U}_{*\mathbf{L}}$ and $\mathbf{U}_{*\mathbf{R}}$ without the middle wave speed can prevent the shock instability problem. Quirk employed the HLLE scheme in the vicinity of strong shock using a localized switching function [1]. We suggest another localized switching method. Using our proposed method, the HLLC scheme is switched to the HLL scheme only in the transverse direction of strong shocks and the magnitude of the additional dissipation is automatically determined. Since the HLL scheme can resolve isolated shock exactly, local application of the dissipative HLL scheme has no adverse effect on the overall resolution of flow fields.

3.1. Modified state data and numerical fluxes in the star region

As shown in Eqs. (1)–(5), the HLLC and HLL fluxes are expressed in a single framework, and they can be determined by the expressions of state data $\mathbf{U}_{*\mathbf{L}}$ and $\mathbf{U}_{*\mathbf{R}}$.

Introducing a switching function f, the new data of states $\mathbf{U}_{*\mathbf{L}}{}^{new}$ and $\mathbf{U}_{*\mathbf{R}}{}^{new}$ are expressed as follows:

$$\mathbf{U}_{*\mathbf{L}}^{new} = f \cdot \mathbf{U}_{*\mathbf{L}}^{+}(1-f) \cdot \mathbf{U}^{HLL}, \tag{17a}$$

$$\mathbf{U}_{*\mathbf{R}}^{new} = f \cdot \mathbf{U}_{*\mathbf{R}}^{+}(1-f) \cdot \mathbf{U}^{HLL}. \tag{17b}$$

The function f has a value of 0.0 or 1.0.

Left and right fluxes in the star region are now defined by newly obtained data of states $\mathbf{U}_{*\mathbf{L}}{}^{new}$ and $\mathbf{U}_{*\mathbf{R}}{}^{new}$:

$$\mathbf{F}^{new}_{*\mathbf{L}} = \mathbf{F}_{\mathbf{L}} + S_L\left(\mathbf{U}^{new}_{*\mathbf{L}} - \mathbf{U}_{\mathbf{L}}\right), \tag{18a}$$

$$\mathbf{F}^{new}_{*\mathbf{R}} = \mathbf{F}_{\mathbf{R}} - S_R\left(\mathbf{U}_{\mathbf{R}} - \mathbf{U}^{new}_{*\mathbf{R}}\right). \tag{18b}$$

The resulting data of states $\mathbf{F}^{new}_{*\mathbf{L}}$ and $\mathbf{F}^{new}_{*\mathbf{R}}$ can be applied directly in the HLLC scheme. This method, named HLLC–HLL, can also be applied to other approximate Riemann solvers.

3.2. Switching function f

We define a function f_p in the form of the inverse of a mesh refinement monitor function [1] to identify the location of shock waves:

$$f_p = \begin{cases} 1.0, & \text{if } \frac{\min(p_R, p_L)}{|p_R - p_L| + \varepsilon} \geqslant 1.0 \\ 0.0, & \text{otherwise}, \end{cases} \tag{19}$$

where ε is chosen to be 10^{-16}. p_L and p_R are pressures which act on the cell interface. The shock instability occurred due to the transferred perturbation in the transverse direction of the shock. Therefore, all the neighboring cells must be examined [15]. The required surfaces for the function f_p in the x-and y-direction are calculated as

$$f_{px} = \min\left(f_{pi+1/2,j}, f_{pi,j+1/2}, f_{pi,j-1/2}, f_{pi+1,j+1/2}, f_{pi+1,j-1/2}\right), \tag{20a}$$

$$f_{py} = \min\left(f_{pi,j+1/2}, f_{pi-1/2,j}, f_{pi+1/2,j}, f_{pi-1/2,j+1}, f_{pi+1/2,j+1}\right). \tag{20b}$$

Except for shock waves, the pressure changes continuously and the pressure difference $p_R - p_L$ across the cell interface is not large. Therefore, the function f_p has a value of 1.0 in most of the computational domain. In the vicinity of the shock waves, the pressure difference is increased and the function f_p has a value of 0.0.

Next, we examine the transverse direction and the shock strength. The resulting switching function f is only applied to the transverse direction of the shock for the case of strong shock as follows:

$$\text{if } f_p = 0.0, \quad f = \begin{cases} 1.0, & \text{if } M_{\mathrm{L}} > 1.0 \text{ and } M_{\mathrm{R}} > 1.0 \\ 1.0, & \text{if } M_{\mathrm{L}} < 1.0 \text{ and } M_{\mathrm{R}} < 1.0 \\ 0.0, & \text{otherwise}. \end{cases} \tag{21}$$

M_L and M_R are local Mach numbers at the cell interface. Wherever the function f has a value of 0.0, the HLLC scheme is switched to the HLL scheme.

3.3. Treatment of the shear waves for the TVD condition in the WAF scheme

Tangential velocity components exist in the multidimensional problem, and they are related to shear waves. For a MUSCL-type scheme, the limiting process of the tangential velocity components is carried out during the reconstruction. However, the WAF scheme is the high-order extension by an integral average of the flux across the full structure of a local Riemann problem. The limiting procedure is applied to each flux component in the Riemann fan. Quirk presented the importance of the shear wave and proposed a "shear fix" for the Roe scheme using the WAF scheme [16]. His results showed that the proper treatment of the shear wave in the Roe scheme can give results as good as those by the exact Riemann solver for the shock reflection problem. Toro suggested a simple approach for the treatment of the shear waves in the WAF scheme [4]. In a two-dimensional system, the y-momentum equation is treated separately by regarding it as a scalar equation.

If the switching function has a value of 0.0, the numerical flux is switched from the HLLC scheme to the HLL scheme, and no limiting is applied to the shear wave. The y-momentum component is calculated in the same manner as Eq. (14). If the function f has a value of 1.0, the y-momentum component is calculated as [4]

$$F^{TVD}_{\rho u_n u_t} = \left[\frac{1}{2}\left(1 + \phi^{(u_t)}\right)u_{tL} + \frac{1}{2}\left(1 - \phi^{(u_t)}\right)u_{tR}\right]F^{TVD}_{\rho u_n}, \tag{22}$$

where $\phi^{(u_t)}$ is a limiter function applied to the tangential velocity component across the v-shear wave in the rotated frame, and $F^{TVD}_{\rho u_n}$ is the TVD flux for the continuity equation. Eq. (22) is also used in the original HLLC scheme.

4. Numerical results

All the numerical computations were conducted using a CFL number of 0.5 except steady normal shock case. Every result in each test problem is printed at the same time level.

4.1. Odd–even decoupling

Fig. 1 shows Quirk's odd–even decoupling test problem [1]. The centerline of the grid is perturbed from a perfectly uniform grid by $\pm 10^{-6}$, and the grid size is 801×21. A moving shock of $M_s = 6.0$ propagates down a duct. The results show the

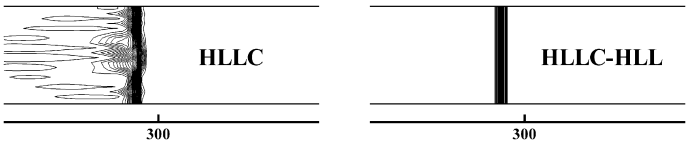

Fig. 1. Odd–even grid perturbation problem: density contours (second-order WAF with MINBEE (Minmod) limiter).

density contour at $X_s \sim 300$. The HLLC scheme shows the promotion of odd–even decoupling along the shock. Using the switching function f, HLLC–HLL shows that decoupling was completely eliminated. The function f was activated only in the transverse direction of the shock.

4.2. Steady normal shock

Fig. 2 shows the results of steady normal shock test case for Mach 20 flow. The grid size is 51×26 and the left (L: $i \leqslant 12$) and right (R: $i \geqslant 14$) conditions across the normal shock are taken from [17]. The intermediate state conditions (M: $i = 13$) are taken from [17,18]. The density at the intermediate state is given as

$$\rho_M = \varepsilon\rho_L + (1-\varepsilon)\rho_R, \tag{23}$$

where the shock position parameter $\varepsilon = 0.0, 0.3, 0.5, 0.7$ and all other variables are calculated to lie on the Hugonoit curve [18]. The top and bottom boundary conditions are given as periodic and the outflow mass flux is fixed to preserve the initial shock position [17]. Chauvat et al. [18] presented a stability diagram on two-dimensional steady normal shock flow for Mach number and shock position parameter. For the Mach number of 20, Godunov, Roe or HLLC schemes showed stable solution from the shock position parameter of 0.64 [18]. Fig. 2 shows similar results to the result of Chauvat et al. The HLLC scheme gives stable solutions for parameter $\varepsilon = 0.0$ and $\varepsilon \geqslant 0.7$ and HLLC–HLL shows stable solutions for all values of ε.

4.3. Carbuncle phenomenon

The carbuncle problem has been observed and discussed for many years, and is considered a typical example of shock instability. When supersonic or hypersonic blunt body flow is simulated, spurious solutions can appear along the stagnation line. There are nonphysical recirculation regions, and a protuberance grows ahead of the bow shock. Fig. 3 shows the numerical results of supersonic circular blunt body flows. The freestream Mach number is 6.0, and the grid size is 401×401. In Fig. 3, the HLLC scheme with the shear wave treatment described in Section 3.3 shows a sawtooth-like shock front, but the typical protuberance did not grow. The spurious solution along the stagnation line is not shown in HLLC–HLL. The switching function was activated ($f = 0$) for only a small portion of the shock region along the transverse direction of the shock wave.

4.4. Kinked mach stem

When a plane shock is reflected from a ramp, a double-Mach reflection (DMR) is formed if the interaction between the shock wave reflection and the shock-induced flow deflection process is strong. When a DMR is formed, the primary Mach stem is sometimes kinked, similar to the carbuncle phenomenon. Fig. 4 shows the numerical results of a kinked Mach stem test problem: a planar moving shock has a speed of $M_s = 5.5$, the ramp angle is 30°, and the grid size is 401×401. The HLLC scheme shows the kinked primary Mach stem. Using the function f, the spurious kinked Mach stem was completely eliminated. The function f caught only strong shock waves, the moving shock, the primary Mach stem, and the end of the curved part of the reflected shock. In addition, the function f was only activated in the numerical flux of the y-direction. There was a

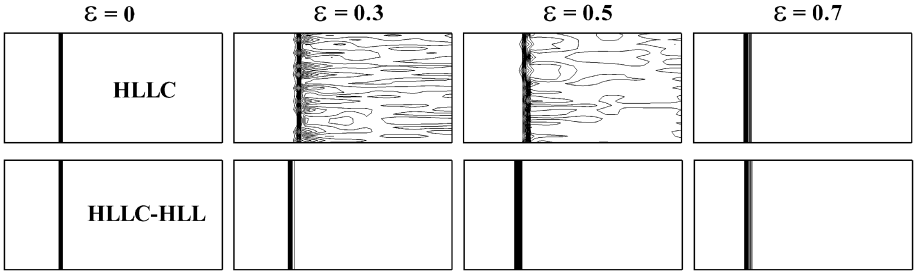

Fig. 2. Steady normal shock test problem: density contours (second-order WAF with MINBEE (Minmod) limiter).

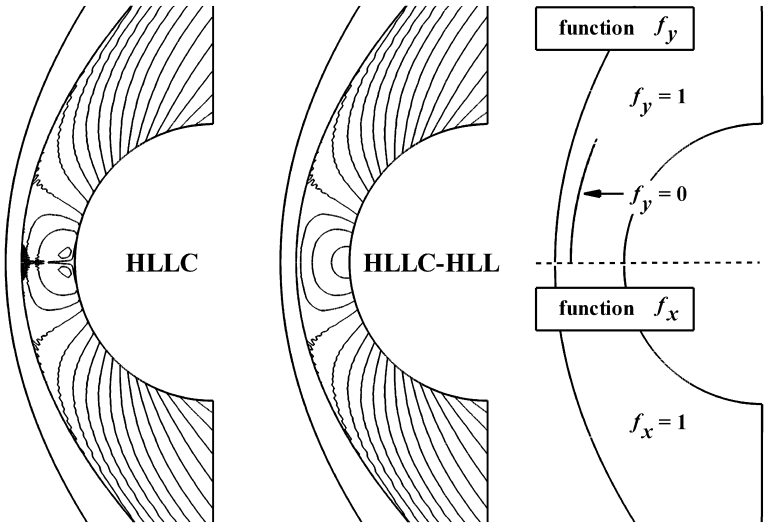

Fig. 3. Supersonic circular blunt body: density and switching function distributions (second-order WAF with MINBEE (Minmod) limiter).

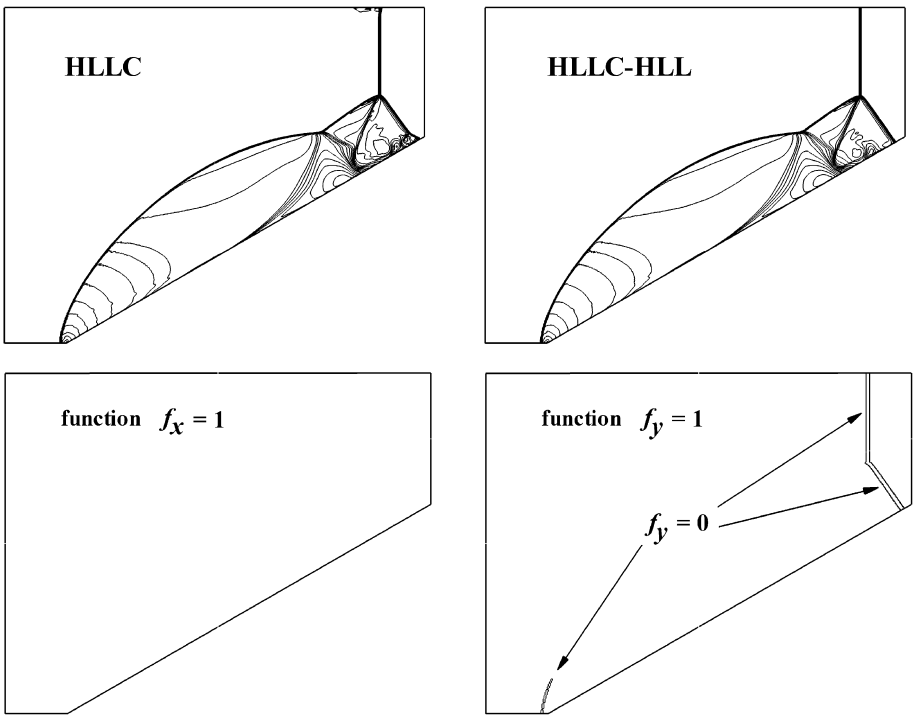

Fig. 4. Kinked Mach stem problem: density and switching function distributions (second-order WAF with MINBEE (Minmod) limiter).

small incipient odd–even decoupling where the incident shock crossed the upper boundary for the HLLC scheme. This was also eliminated by the HLLC–HLL.

4.5. Supersonic corner flow

Fig. 5 shows the results of a supersonic corner problem. A moving shock with $M_s = 5.09$ diffracts around a 90° corner. The grid size is $201 \times 201 + 401 \times 401$. The HLLC scheme showed no problem at the corner, but spurious oscillations were observed at the planar moving shock. The switching function f was activated on the step corner and moving shock waves. Using the function f, the spurious solutions along the planar moving shock were completely eliminated.

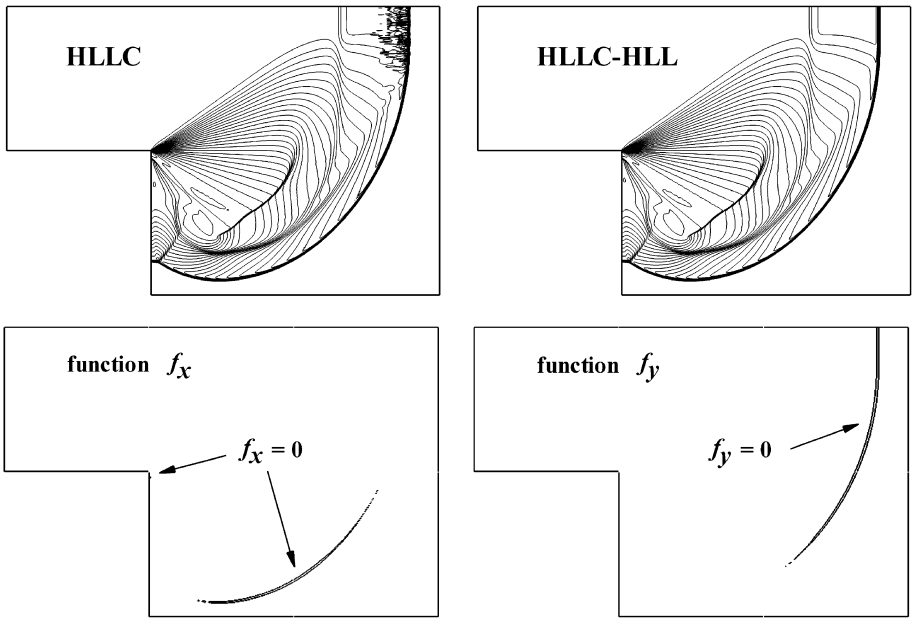

Fig. 5. Supersonic corner flow: density and switching function distributions (second-order WAF with MINBEE (Minmod) limiter).

5. Conclusion

The approximate Riemann solvers which resolve contact and shear waves can give unphysical results in the presence of strong shock waves. Many numerical methods which add dissipation have been reported to prevent such failures. We proposed another way of adding dissipation to the HLLC scheme. Among the reliable approximate Riemann solvers, the HLL scheme can resolve the isolated shock waves exactly with exact wave speed estimation, and it can be easily combined into the HLLC scheme. Since so-called shock instability is due to perturbation transfer in the transverse direction of a strong shock, the HLL scheme is applied in this direction. To identify a strong shock and the transverse direction of the shock, an appropriate switching function was defined and presented in this paper. This has the same effect as adding dissipation to the transfer direction of the perturbation, and the magnitude of the additional dissipation is automatically determined. For a high-order extension using the WAF scheme, the treatment of the v-shear wave is modified in the framework of Toro's suggestion.

The resulting method was tested against a steady normal shock instability problem and Quirk's test problems. Odd–even decoupling, steady normal shock, the carbuncle phenomenon, DMR flows, and supersonic corner flows were successfully stabilized with our method. The dissipative scheme was used in a small portion of the shock region along the transverse direction of the strong shock wave. Since the HLL scheme can resolve isolated shock exactly, local application of the dissipative HLL scheme had no adverse effect on the overall resolution of flow fields.

Acknowledgments

This work was supported by the second stage of the Brain Korea 21 Project in SNU and the Korea Science and Engineering Foundation (KOSEF) grant funded by the Korea government (MEST) (No. R01-2008-000-12362-0). The authors would like to acknowledge the support from KISTI (Korea Institute of Science and Technology Information) under [The 7th Strategic Supercomputing Support Program] with Dr. Woo Jun as the technical supporter. The use of the computing system of the Supercomputing Center is also greatly appreciated.

References

[1] J.J. Quirk, A contribution to the Great Riemann solver debate, Int. J. Numer. Meth. Fluid 18 (1994) 555–574.
[2] M.S. Liou, Mass flux schemes and connection to shock instability, J. Comput. Phys. 160 (2000) 623–648.
[3] A. Harten, P.D. Lax, B. van Leer, On upstream differencing and Godunov-type schemes for hyperbolic conservation laws, SIAM Rev. 25 (1983) 35–61.
[4] E.F. Toro, Riemann solvers and numerical methods for fluid dynamics, second ed., Springer, 1999.
[5] B. Einfeldt, C.D. Munz, P.L. Roe, B. Sjogreen, On Godunov-type methods near low density, J. Comput. Phys. 92 (1991) 273–295.
[6] E.F. Toro, M. Spruce, W. Speares, Restoration of the contact surface in the HLL-Riemann solver, Shock Waves 4 (1994) 25–34.
[7] P. Batten, N. Clarke, C. Lambert, D.M. Causon, On the choice of wavespeeds for the HLLC Riemann solver, SIAM J. Sci. Comput. 18 (1997) 1553–1570.
[8] S.D. Kim, B.J. Lee, H.J. Lee, I.-S. Jeung, J.-Y. Choi, Realization of contact resolving approximate riemann solvers for strong shock and expansion flows, Int. J. Numer. Method Fluid, doi:10.1002/fld.2057.

[9] E.F. Toro, A weighted average flux methods for hyperbolic conservation laws, Proc. R. Soc. Lond. A 423 (1989) 401–418.
[10] E.F. Toro, The weighted average flux method applied to the Euler equations, Philos. Trans. R. Soc. Lond. A 341 (1992) 499–530.
[11] S.J. Billett, E.F. Toro, On WAF-type schemes for multidimensional hyperbolic conservation laws, J. Comput. Phys. 130 (1997) 1–24.
[12] S.J. Billett, E.F. Toro, Unsplit WAF-type schemes for three dimensional hyperbolic conservation laws, in: E.F. Toro, J.F. Clarke (Eds.), Numerical Methods for Wave Propagation, Kluwer Academics Publishers, 1998, pp. 75–124.
[13] D. Drikakis, W. Rider, High-resolution Methods for Incompressible and Low-speed Flows, Springer, 2005.
[14] M. Pandolfi, D. D'Ambrosio, Numerical instabilities in upwind methods: analysis and cures for the Carbuncle phenomenon, J. Comput. Phys. 166 (2001) 271–301.
[15] S.S. Kim, C. Kim, O.H. Rho, S.K. Hong, Cure for the shock instability: development of a shock-stable Roe scheme, J. Comput. Phys. 185 (2003) 342–374.
[16] J.J. Quirk, An Adaptive Grid Algorithm for Computational Shock Hydrodynamics, Cranfield Institute of Technology, Ph.D. Thesis, 1991.
[17] K. Kitamura, P.L. Roe, F. Ismail, An Evaluation of Euler Fluxes for Hypersonic Flow Computations, in: 18th AIAA Computational Fluid Dynamics Conference, AIAA paper 2007-4465, 2007.
[18] Y. Chauvat, J.-M. Moschetta, J. Gressier, Shock wave numerical structure and the carbuncle phenomenon, Int. J. Numer. Meth. Fluid 47 (2005) 903–909.